1. LEG 78B: BACKGROUND, OBJECTIVES, AND GEOLOGICAL SETTING[1]

Matthew H. Salisbury, Deep Sea Drilling Project, Scripps Institution of Oceanography
and
Roy D. Hyndman, Pacific Geoscience Centre, Department of Energy, Mines and Resources, Sidney, B. C.[2]

BACKGROUND AND OBJECTIVES

During the past several years, increased recognition of the scientific potential of deep-sea boreholes as conduits for conducting geophysical research in the crust has led to greater emphasis on downhole measurements and experiments by the Deep Sea Drilling Project. The importance of such experiments arises mainly from the need to integrate data from a wide variety of sources—including downhole logs and experiments, geophysical and geological site surveys, and studies of core material—in order to understand the structure and physical properties of the crust.

Although the concept of an integrated program of coring followed by downhole measurements and experiments is relatively new, the Deep Sea Drilling Project has already gained considerable experience with individual measurements and experiments. A limited downhole logging program was conducted on Legs 1 through 6, employing natural-gamma, gamma-density, neutron-porosity, and resistivity tools operated by personnel from Grice Ocean Engineering, Schlumberger, and Dresser-Atlas. After a long hiatus, the logging program was renewed in 1974 and has continued on many, although not all, cruises since that time, using personnel and equipment provided by Schlumberger and Gearhart-Owen. The tools have included those listed above, plus sonic velocity, temperature, and caliper logs. Although the quality of the data has occasionally been excellent (e.g., Legs 48, 61, 69, and 70; Montadert, Roberts, et al., 1979; Boyce, 1981; Cann and Von Herzen, 1983), many of the logs have suffered from poor hole conditions, operational difficulties, and tool problems. In general, good logs were obtained only by persistence.

A limited heat-flow program has also been carried out on the *Glomar Challenger* since the beginning of the project to measure temperature and heat flow as a function of depth in the sediment column and to monitor transient thermal phenomena. Although the importance of such measurements is widely recognized and the tools have gone through changes and developments, the number of valid measurements remains small (see review by Hyndman et al, this volume).

With the expansion of the drilling program to include major basement or crustal objectives during the International Phase of Ocean Drilling (IPOD), several geophysicists began to design downhole experiments for studying the ocean crust and to deploy them from the *Challenger.* These included an oblique seismic experiment, in which a downhole seismometer is lowered and monitored from the drill ship while a shot pattern is detonated from a second ship (successfully deployed on Legs 52, 65, and 70; Stephen et al., 1980, 1983; Stephen, 1983); a long-term borehole-recording seismometer experiment designed to monitor natural seismicity and explosions (successfully deployed on Leg 67; Aubouin, von Huene, et al., 1982); a large-scale resistivity experiment designed to investigate the electrical resistivity of the formation beyond the zone invaded by drilling fluids (Legs 60 and 70; Francis, 1982; Von Herzen et al., 1983); and a combined downhole packer-televiewer experiment designed to measure permeability, fluid flow, pore pressure, and *in situ* stress in the crust (Leg 69; Zoback and Anderson, 1983).

In general, these experiments have been conducted separately on cruises having other primary objectives. When several of these experiments were very successfully combined with logging on Legs 51–53, 69, and 70 (Salisbury et al., 1980), it was realized that there would be considerable value in conducting cruises with logging and downhole experiments, rather than coring, as the primary objectives.

Leg 78B represents the first such cruise specifically designed and approved by the JOIDES advisory panels for downhole measurements. The original impetus for the cruise arose from the scarcity of good downhole logs in the ocean crust. This was particularly critical in the few deep crustal holes drilled, because the recovery in such holes was poor and because the physical properties of the core material were clearly not representative of the large-scale properties of the crustal sections penetrated. One of the deepest of these holes, and one of the most attractive candidates for re-entry (since it had been cased to basement) was Hole 395A on the Mid-Atlantic Ridge (Fig. 1). The hole had been drilled on Leg 45 (Melson, Rabinowitz, et al., 1979a) to a sub-basement depth of 571 m in 7.2-Ma-old crust on the west side of the ridge, south of the Kane Fracture Zone, as part of a long-term program designed to determine the petrological, geochemical, and geophysical properties of the ocean crust and to determine the mechanisms by which it forms and evolves. Although the hole had been continuously

[1] Hyndman, R. D., Salisbury, M. H., et al., *Init. Repts. DSDP*, 78B: Washington (U.S. Govt. Printing Office).
[2] Addresses: (Salisbury) Deep Sea Drilling Project, Scripps Institution of Oceanography, La Jolla, CA 92093; (Hyndman) Pacific Geoscience Centre, Dept. of Energy, Mines and Resources, P.O. Box 6000, Sidney, B. C. V8L4B2, Canada.

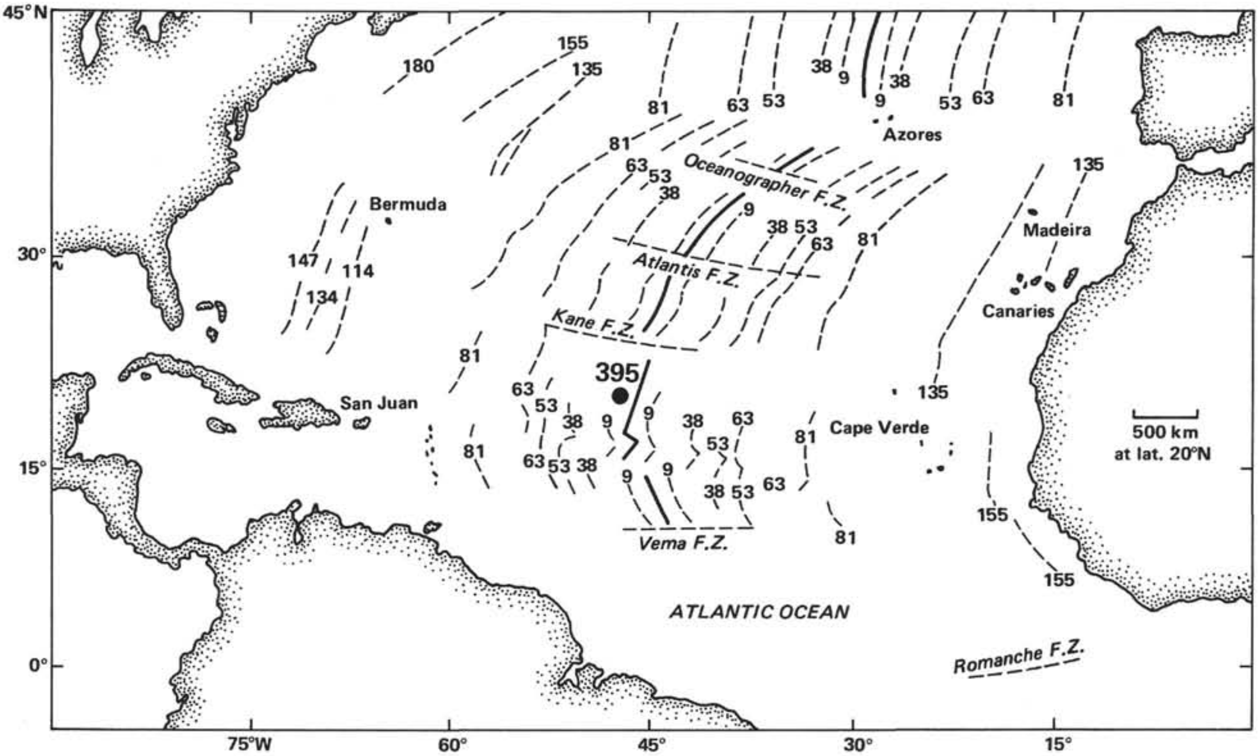

Figure 1. Location of Hole 395A. Dashed lines show age of the crust in Ma, deduced from magnetic anomalies.

cored and the recovered material extensively studied, no downhole measurements had been made, and the core recovery was poor. In consequence, many important features of the drilled section, such as its velocity structure and formation properties, remained obscure.

Detailed regional geophysical data from this area were already available from the original site surveys carried out before drilling (Hussong et al., 1979; Purdy et al., 1979; Kasahara et al., 1980; Rabinowitz and Ludwig, 1980). These studies included detailed bathymetry, magnetics, gravity, seismic reflection (including multichannel) profiling, seismic refraction data from ocean-bottom seismographs and sonobuoys, and several heat-flow measurements. At the same time, the stratigraphy of the hole and the petrology, geochemistry, and physical properties of the rocks were known from studies of the core and from the drilling record (Melson, Rabinowitz, et al., 1979b). Important results that still needed to be corroborated and investigated in detail included a marked disparity in regional versus laboratory seismic velocities, which implies large-scale porosity; magnetic reversals in the core, which may imply short-duration field reversals or long-distance lava transport; and very low regional heat-flow values, which may imply vigorous circulation and thus high permeability in the crust.

The primary objective of the Leg 78B scientific program was therefore to study the geophysical and hydrogeological properties of the upper oceanic crust at Site 395 through downhole logging and downhole experiments, for comparison with previous studies of the core and with regional geophysics. For a general understanding of the structure and physical properties of the crust and of the processes affecting it, these measurements must be conducted at many scales of investigation. Site survey data are needed to determine the regional properties of the crust; downhole measurements and experiments are needed to provide information on a wide variety of properties under *in situ* conditions at a scale of investigation of a few meters; and laboratory measurements on core samples are needed to define the intrinsic behavior of the materials making up the crust. Although laboratory measurements allow calibration of the downhole logs, they do not usually give results representative of the formation, because of the small size of the samples studied, because of serious core-recovery biases, and because of the difficulty of simulating *in situ* conditions in the laboratory. The differences, however, between laboratory and logging results and between the results of logging and regional geophysical studies give important information on the nature and extent of cracks, fissures, and other forms of large-scale porosity in the crust.

On Leg 78B, it was planned to use logging tools designed to measure the diameter of the hole, the temperature of the water in the hole, and the sonic velocity, electrical resistivity, bulk density, porosity, and natural gamma radiation of the formation. Additional special downhole tools included a borehole acoustic televiewer designed to outline structures in the wall of the hole (such as pillows, flows, and fractures) and a downhole magnetometer/susceptibility meter designed to measure field variations associated with differences in rock magnetization direction and intensity (particularly those associated with field reversals) and to measure differences in the intrinsic magnetic properties of the rocks.

The downhole experiment program was planned to include (1) a packer experiment for large-scale permeability tests, *in situ* pressure tests, large-volume water sampling, and hydrofracture tests; (2) a program to measure the temperature and collect water samples down the hole using the self-contained heat-flow/pore-water sampler; (3) a large-scale resistivity experiment; and (4) the experimental emplacement of a borehole seismometer designed by Teledyne Geotech, Inc. for the Defense Advanced Research Projects Agency (DARPA) and the Naval Ocean Research and Development Activity (NORDA). The seismometer emplacement was intended as a test of the procedures and equipment to be used during the emplacement of a semipermanent seismometer in the floor of the North Pacific by the *Glomar Challenger* in 1982. It was also planned to have a second ship, the *Lynch*, rendezvous at the site to assist in the deployment by providing current-meter measurements and to detonate a pattern of shots to be recorded both by the downhole seismometer and by an array of ocean-bottom seismographs deployed around the site. Thus, an active seismic experiment similar to the oblique seismic experiments conducted on earlier legs was planned as part of the DARPA/NORDA test to complement the other experiments and logs conducted at the site.

GEOLOGICAL AND GEOPHYSICAL SETTING

Site 395 is at 22°45′N, 46°05′W on the west flank of the Mid-Atlantic Ridge about 110 km west of the rift valley and an equal distance south of the Kane Fracture Zone (Figs. 1 and 2). To the east, between the site and the rift, lies the high plateau or crest range described by van Andel and Bowin (1968) and characterized by relatively low relief and water depths of about 3 km.

The region in the vicinity of the site is characterized by high relief (2400–4600 m water depths) with a crude topographic lineation striking N10°E. In addition to a series of regional surveys conducted in the area during the 1960s by the Lamont-Doherty Geological Observatory (*Vema* 2501 and 2503) and the Woods Hole Oceanographic Institution (*Chain* 44; van Andel and Bowin, 1968), the area around the site was surveyed in detail in 1974 by the Hawaii Institute of Geophysics (*Kana Keoki* 74-01-09, Leg 7) as part of the IPOD site survey program, to select a site suitable for deep basement penetration (Hussong et al., 1979; Purdy et al., 1979; Kasahara et al., 1980). Also, Digicon, Inc. ran a multichannel seismic line (Fig. 3) over the site in 1974 to determine whether sub-basement structures could be discerned in the ocean basins using multichannel techniques. These surveys indicate that sediments are present only in isolated ponds occupying topographic depressions (Figs. 3A, 3B, and 4).

Site 395 itself is at the foot of a 1300-m scarp near the edge of one of the youngest and thickest of these ponds. As can be seen in Figure 5, the sediments range up to 0.3 s (2-way travel time) or 300 m in thickness in the southeast portion of the pond. Like many of these ponds, this one shows evidence—in the form of offsets in the sediments across minor faults—of fairly recent tectonic activity. The activity appears to have been limited, however, to the northeast limb, leaving the rest of the pond, including the area around the site, undisturbed.

From analyses of the magnetic anomalies mapped in the area during the site survey program (Fig. 6), it is apparent that Site 395 lies within Anomaly 4 (Figs. 2 and 5). Thus, the crust should have formed about 7.2 Ma ago (Fig. 7) at a half-spreading rate of 1.7 cm/y., and the rocks should be normally polarized (Hussong et al., 1979; Purdy et al., 1979). It should be emphasized, however, that the anomalies are quite variable throughout the area and are difficult to correlate. Although the anomalies, like the bathymetry, display a prominent grain striking N10°E, offsets in the anomaly pattern suggest the presence of small fracture zones north and south of the site (Fig. 7). The more northerly of the two is also suggested by the bathymetry.

During the site survey conducted before drilling, an extensive series of heat-flow measurements was made in and around the site sediment pond to characterize the thermal regime of the site (Fig. 5). Excluding one measurement which appeared anomalously high (120 mW/m^2), all the values fell within 4 mW/m^2 of the site average of 37 mW/m^2. Although this average appears to be low, given the age of the site, the uniformity of the measurements suggests that it accurately represents the heat flow in the pond. If this is so, the heat flow would appear to be depressed by convection in the underlying crust.

In addition to bathymetric and magnetic surveying, a survey of the gravity field was conducted in the area of the site. Although the gravity anomalies shown in Figure 8 have not been modeled in detail, it is apparent from a comparison with Figure 4 that they are closely related to bathymetry.

Finally, a detailed seismic refraction experiment was conducted around the site (Fig. 9) before drilling to determine whether the velocity structure was typical of young ocean crust, and to provide a basis for comparison with the drilling results (Hussong et al., 1979; Kasahara et al., 1980). As can be seen in Table 1 and Figure 10, the layer thicknesses and velocities are highly variable throughout the region even after topographic corrections have been applied to the data: In general, the layers beneath the sediment ponds are thinner and deeper and display higher velocities than equivalent layers beneath topographic highs (Hussong et al., 1979). Similarly, though the 3-layer model of Raitt (1963) is generally applicable, the high-velocity basal layer of Sutton et al. (1971) was observed on at least one of the lines (f in Fig. 10), and the mantle was not observed on another (line d).

Despite these irregularities, however, Layer 2 was reliably detected and surprisingly uniform, at least in velocity, on most lines (V_p ranges from 4.36 to 4.93 km/s, and the thickness ranges from 0.6 to 2.2 km). More particularly, the velocity structure under the pond itself was determined with some certainty because lines c and g (Fig. 10) had reverse refraction directions and could be treated as a single end-to-end reverse profile. The results of this treatment (Fig. 11) indicate that the boundary between Layers 2 and 3 is about 1.3 km below the mudline, the Mohorovičić discontinuity is remarkably shal-

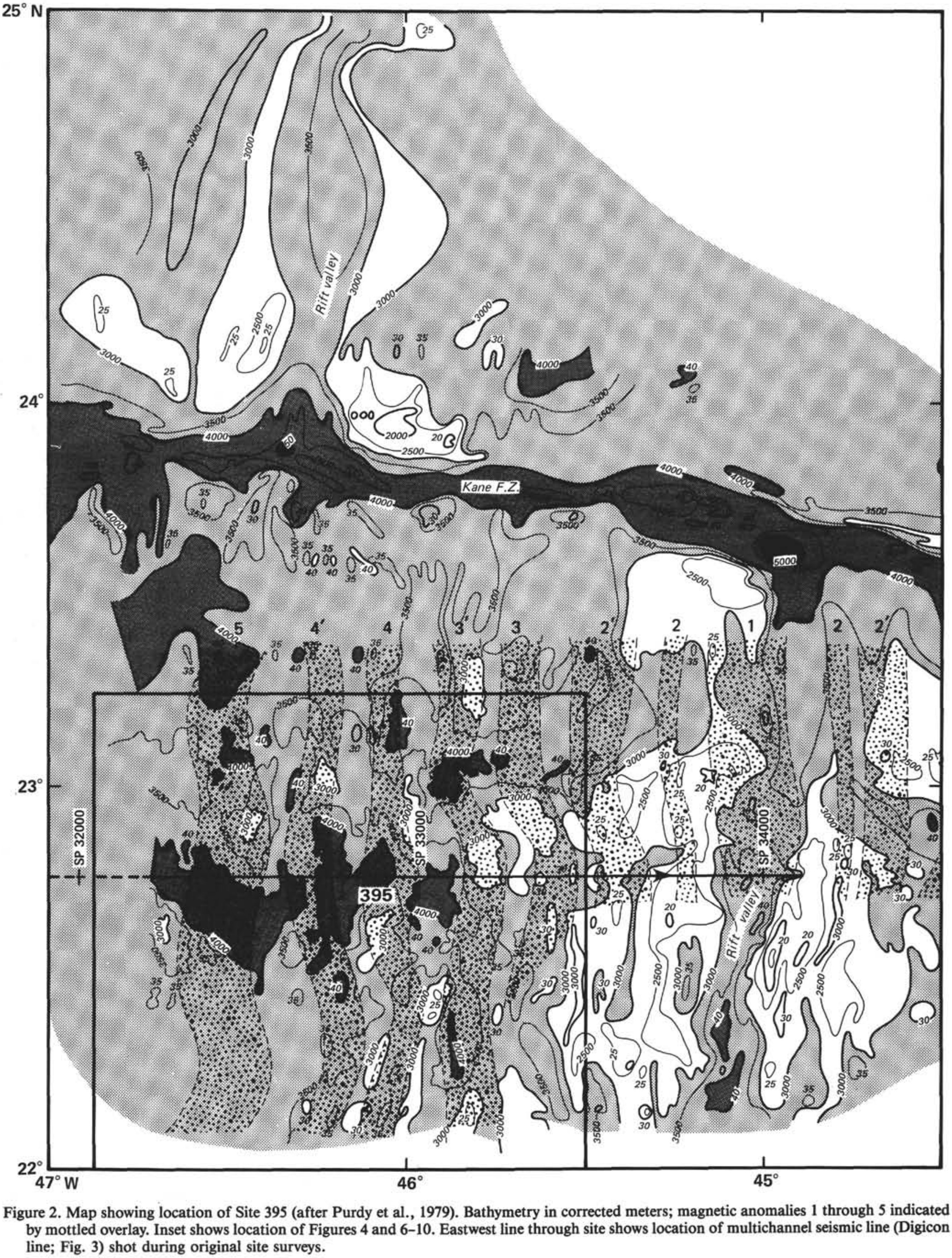

Figure 2. Map showing location of Site 395 (after Purdy et al., 1979). Bathymetry in corrected meters; magnetic anomalies 1 through 5 indicated by mottled overlay. Inset shows location of Figures 4 and 6–10. Eastwest line through site shows location of multichannel seismic line (Digicon line; Fig. 3) shot during original site surveys.

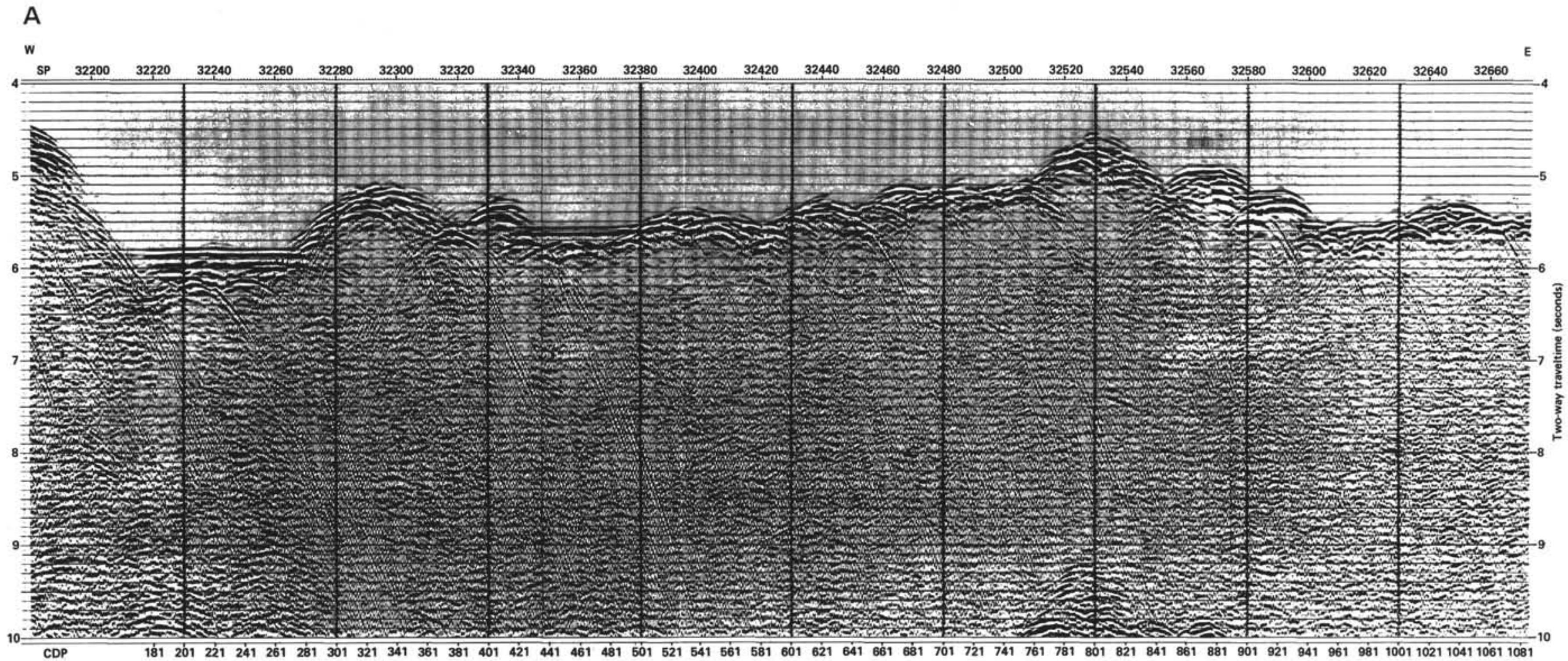

Figure 3. A–D. Dip-filtered multichannel seismic reflection profile (Digicon line) shot along E–W profile over Site 395 by *Gulf Seal*, November, 1974. The profile shown extends from 46°45′W to the east side of the rift valley at 44°54′W (solid line in Fig. 2). (SP = shot point; CDP = common depth point.)

B

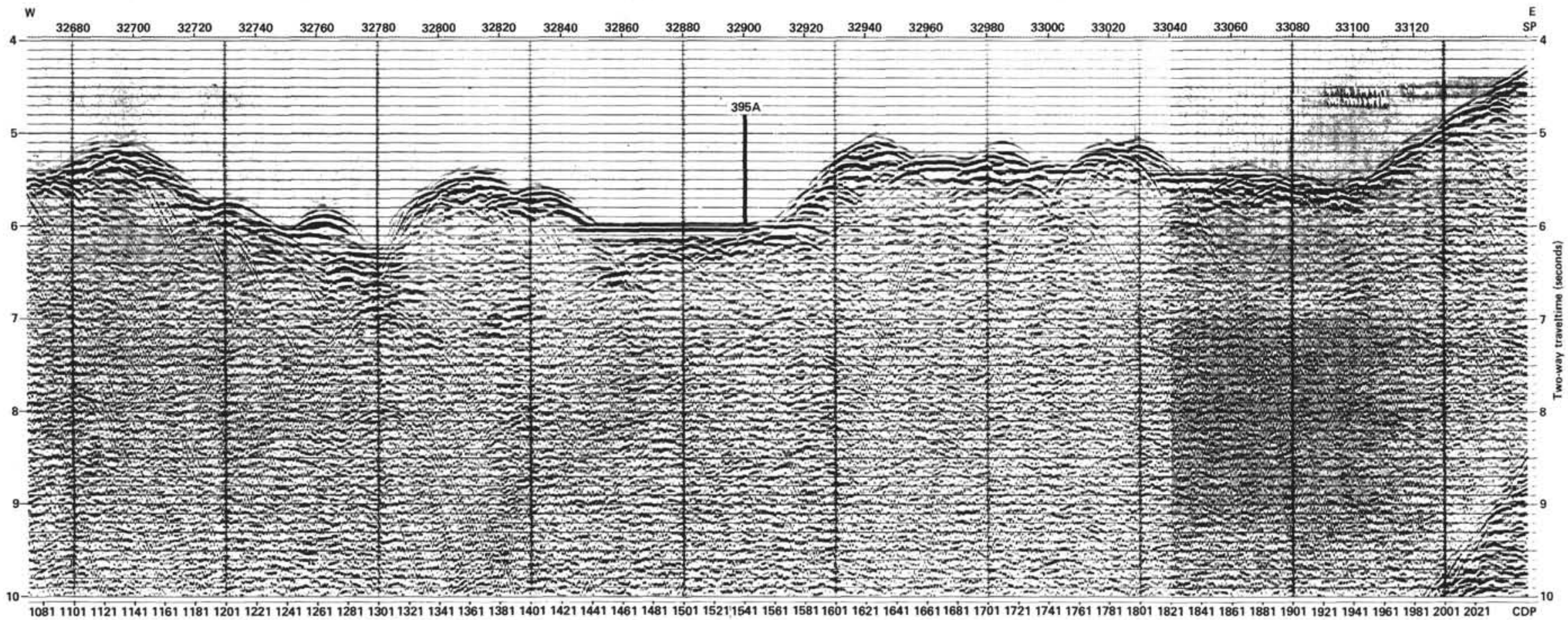

Figure 3. (Continued).

C

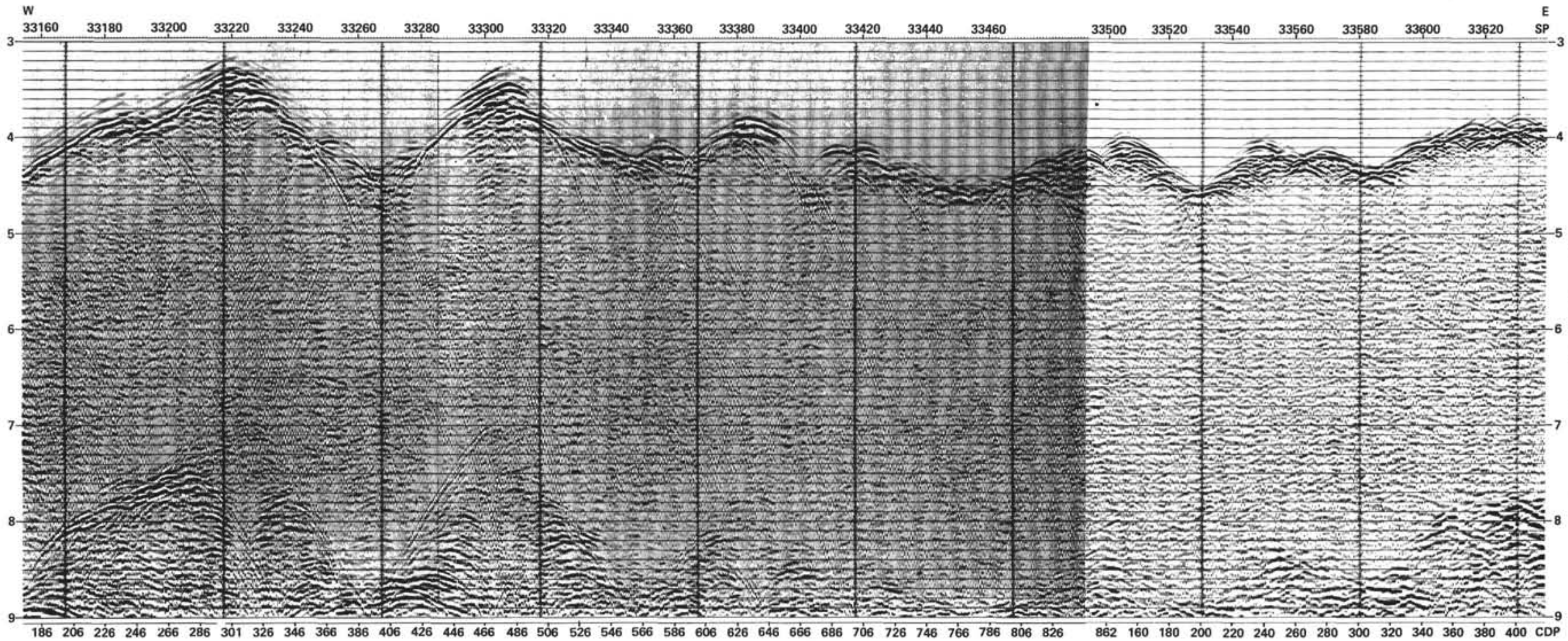

Figure 3. (Continued.)

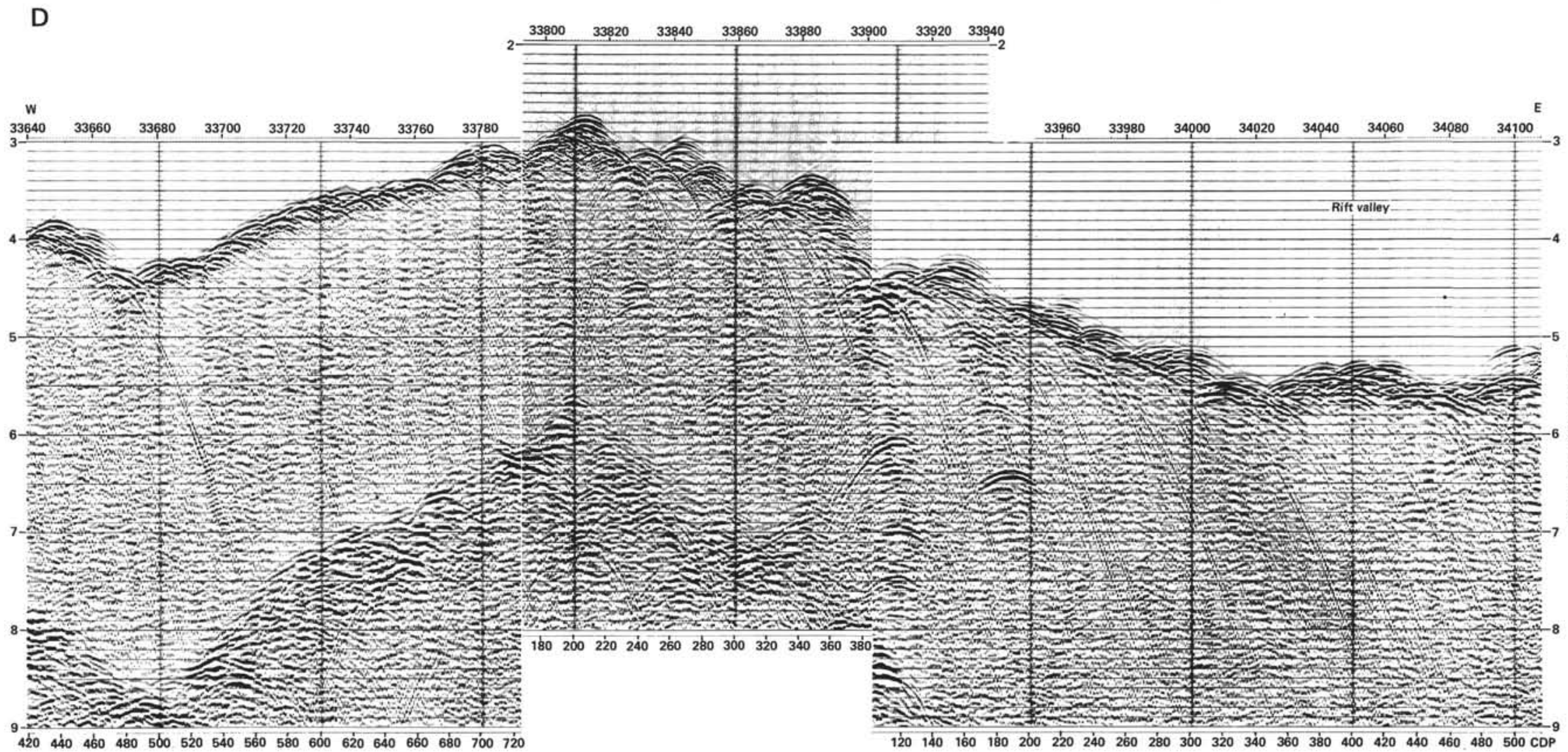

Figure 3. (Continued.)

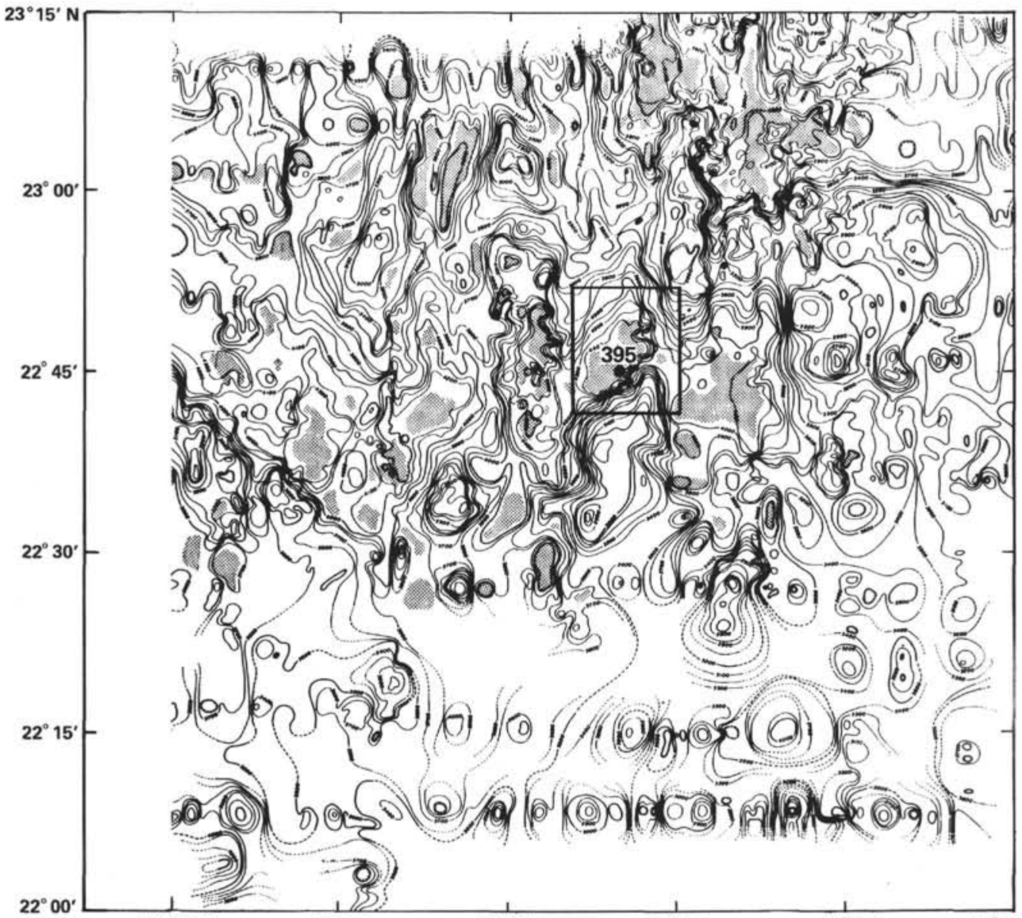

Figure 4. Detailed bathymetry (in corrected meters) in the vicinity of Site 395 (after Hussong et al., 1979). Stippled areas indicate sediment ponds. Inset shows location of Figure 5.

low—above 4 km sub-bottom—and the velocities of Layers 2 and 3 and the mantle are 4.6, 6.4, and 8.2 km/s, respectively (Kasahara et al., 1979). It should be noted, however, that the relief on the steep (17°) scarp immediately to the southeast of the site is comparable to or greater than the depth to Layer 3, and that the apparent Layer-3 velocities shown in this direction (7.4 km/s on line d in Fig. 10) are exceptionally high. If this scarp is a fault scarp, it is possible that plutonic rocks are exposed at the surface. Although the Digicon line clarifies the shape of the sediment basin at Site 395 (Fig. 3B), no sub-basement structures suggesting such a relationship were observed.

HOLE 395A

Hole 395A was drilled on Leg 45 to a sub-bottom depth of 664 m, 571 m of which was in basement. The hole took 31 days to drill (9 December 1975 to 9 January 1976), including setting the re-entry cone and casing and making six bit changes.

The sediment section, which was cased, consists of 93 m of Pleistocene to upper Miocene foraminiferal-nannofossil ooze interbedded with foraminiferal sands and laced with turbidites containing fragments and shards of basalt and serpentinite. This was underlain by 18 m of rubble, presumably talus from the scarp to the southeast, composed of clasts and cobbles of basalt, gabbro, and serpentinite in an ooze matrix. The remainder of the section, from the base of the rubble to the bottom of the hole, consists of pillow basalts (509 m or 89% of the section), intrusive dolerites (22 m; 4%), igneous breccias (40 m; 7%), and traces of serpentinite. No interbedded sediments were recovered.

As can be seen in Table 2 and Figure 12 (Melson, Rabinowitz, et al., 1979b; Natland, 1979), the basement section can be divided into 23 lithologic units belonging to eight major chemical units plus a serpentinite breccia below the uppermost extrusive. The chemical units consist of three aphyric pillow basalt units (A_2, A_3, and A_4) and five phyric units (P_2, P_3, P_4, $P_4{}'$, and P_5), of which P_2 is massive and $P_4{}'$ is the intrusive equivalent of P_4. Each chemical unit (if P_4 and $P_4{}'$ are taken together) appears to represent a discrete episode of submarine volcanism. On geochemical and magnetic grounds it appears that few, if any, of these units are comagmatic or related to each other by fractionation, even though all are low-K tholeiites.

The uppermost unit, A_2 (111–173 m sub-bottom), is the least fractionated of the aphyric units. It is a normally polarized pillow basalt with an average inclination

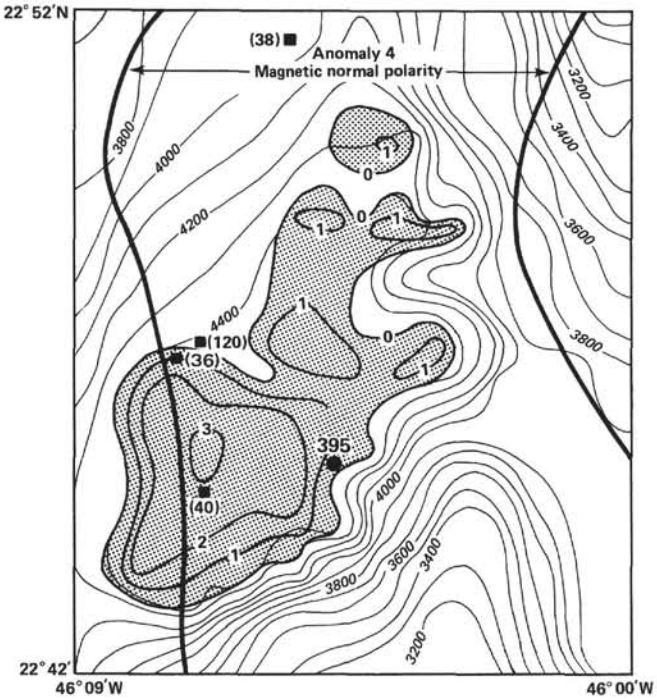

Figure 5. Detailed bathymetry (in corrected meters) and sediment isopach map (sediment thickness in tenths of a second two-way travel time) in the immediate vicinity of Site 395 (after Purdy et al., 1979). Also shown are the boundaries of magnetic Anomaly 4 and the locations of heat-flow stations (sqares) and their values (in parentheses) discussed in the text.

of +38°, which is consistent with the expected inclination for the site (+40°) and the observed polarity of Anomaly 4. The inclination and intensity of magnetization are extremely regular, suggesting that the entire 62-m thick unit was extruded within less than 100 yrs.

Immediately beneath Unit A_2 is an 8-m-thick breccia composed of basalt and serpentinite clasts. The unit is equivalent to a more complex breccia found at an equivalent sub-basement depth in Hole 395, and is thought to represent a talus deposit similar to the rubble overlying Unit A_2.

The next four units (181–362 m sub-bottom) consist of phyric basalt. The uppermost, Unit P_2, is a 29-m-thick unit of plagioclase–olivine phyric basalt. The only massive extrusive unit in the section, it is normally polarized (+20 to +40°), and is the most evolved of the phyric basalts. The remaining three phyric units, P_3, P_4, and P_5, are 50, 48, and 54 m thick, respectively, and consist of plagioclase–olivine ± clinopyroxene phyric pillow basalts with glassy selvages throughout and breccias near the base of the sequence. Unit P_3 is normally polarized (+40 to +50°), but P_4 and P_5 are reversely polarized (−38 and −40°, respectively). The top of Unit P_4 is more weathered than the base of P_3, and no transitional orientations were observed between the two, suggesting a hiatus between eruptions longer than a typical magnetic polarity transition. Units P_3, P_4, and P_5 are successively more evolved with depth, with P_3 the most primitive phyric basalt in the section.

The next unit, A_3 (362–570 m sub-bottom), is a 208-m-thick reversely polarized (−43°) aphyric pillow basalt

Table 1. Seismic refraction results near Site 395.

Receivers	2 Velocities (km/s)	3	4	Water depth (km)	2 Thickness (km)	3
4				3.51	1.37	1.77
	3.78	6.46	7.43			
3				3.95	1.44	2.52
3				3.93	1.57	
	4.54	6.53	7.91			
2				4.11	1.32	2.18
3				3.76	1.89	
	4.61	6.60	7.71			
OBSI				4.62	0.98	2.60
2	4.86	6.85	7.64	3.95	1.80	2.83
OBSI	4.76	6.78	7.87	4.69	0.84	
5				3.99	1.17	1.44
	3.65	5.95	7.91			
1				3.38	0.90	2.54
1	3.91	6.42	7.45	3.25	1.48	4.14
6	4.65	7.04		3.96	1.73	
7	4.35	5.93	8.53	2.66	1.68	1.59
8				2.70	1.93	5.30(?)
	4.75	6.91				
OBSI				4.64	0.56	2.86
9				4.38	1.19	2.63
	4.53	6.63	8.30			
OBSI				4.71	0.67	2.87
11				3.76	1.18	
	3.79	6.52				
3				4.07	1.46	
3	4.53	7.11	8.39	3.94	1.74	3.36
12	3.84	6.16		3.99	1.59	1.78
13				3.81	1.23	3.67
	4.56	6.70	7.80			
OBSI				4.57	0.98	2.50
OBSI				4.64	1.02	
	4.72	6.79				
6				3.95	0.91	
6	4.39	6.56		3.67	1.79	
14	3.23	4.90	6.12	3.12	0.42	2.26
14						
12						
12	4.40	6.82		4.46	1.38	
3						
15				3.52	0.74	3.81
	3.49	6.39	6.87			
12				4.12	1.68	
15				3.49	0.89	3.70
	3.66	6.46	6.87			
3				4.27	1.31	
12	3.50	6.88		4.19	1.35	
3	3.50	7.27		3.90	1.72	
16				3.40	1.83	2.33
	4.46	6.44	8.09			
OBSI				4.66	0.92	2.30
OBSI	4.41	5.95	8.08	4.73	0.89	2.31

Note: Data taken from Hussong et al. (1979). Numbers 2–4 = Layers.

with breccias at the top and again at about two-thirds of the way down the unit. Starting about midway through this unit (476 m) and continuing to the base of the hole, the section becomes increasingly annealed by low-temperature vein fillings composed of clay, carbonate, zeolites, and traces of opal. Also starting in this unit and continuing intermittently to the bottom of the hole was a marked tendency for the more coherent cores to self-destruct into numerous fragments after recovery. Whether this was a result of stress relief or the expansion under

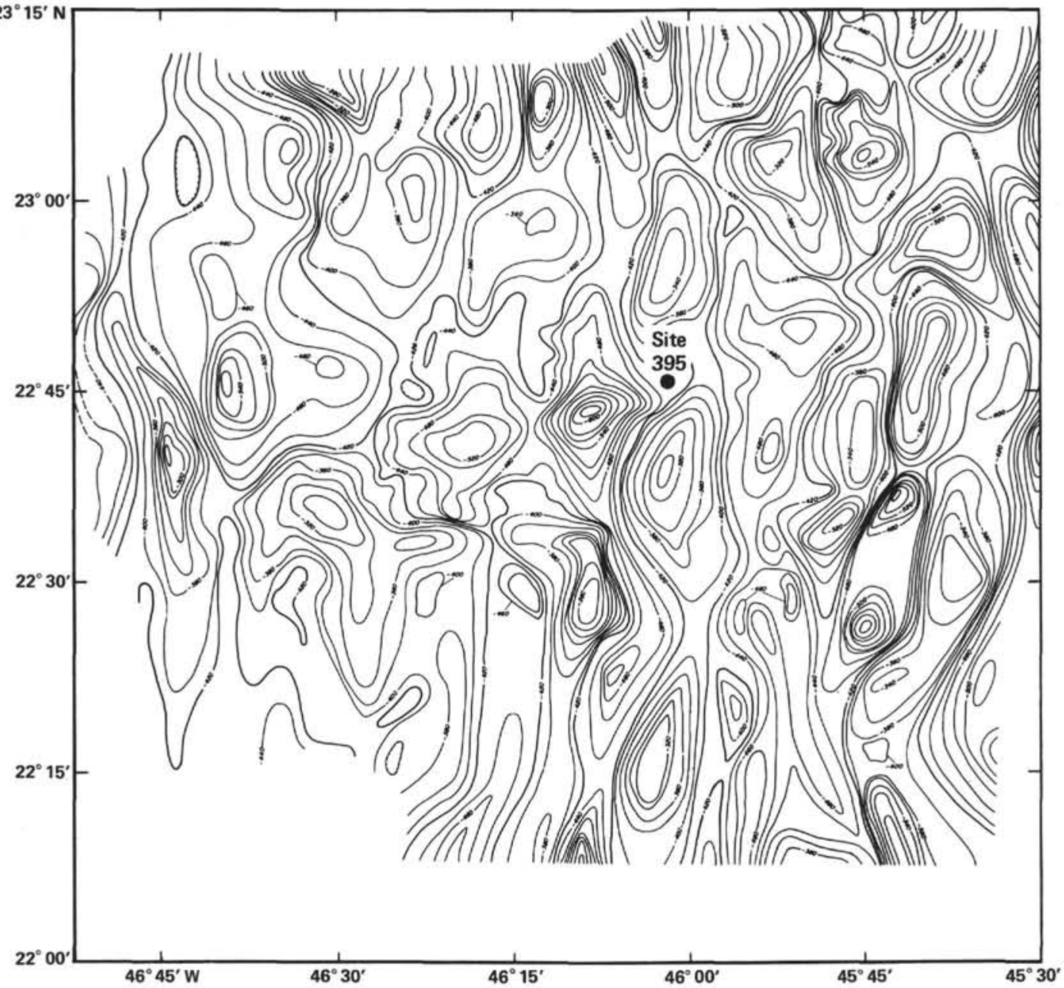

Figure 6. Residual magnetic anomaly map in the vicinity of Site 395 (from Hussong et al., 1979). Total magnetic field intensity shown in gammas after correction for 1965 International Geomagnetic Reference Field.

decompression, of gas, water, or clay in cracks is unknown. The phenomenon was particularly striking in Lithologic Units 18, 21, and 23, and was also observed at about the same depth in Hole 418A.

The deepest aphyric unit (A_4; 570–616 and 633–671 m sub-bottom), consists of an annealed pillow basalt cut by an intrusive dolerite (P_4'; 616–633 m) and interlaced with altered breccias. The unit can be distinguished from A_3 by a subtle change in chemistry and an abrupt change to normal polarity (+50 to +60° above the intrusive). The dolerite is reversely polarized (−40°) and chemically indistinguishable from Unit P_4, which suggests that it is its intrusive equivalent. Below the intrusive, the pillow basalts of Unit A_4 have been hydrothermally altered, causing the intensity of magnetization to decrease and the inclination to become irregular (−60° to +30°) to the base of the hole.

Although the units defined here have been described with an air of certainty (for more detail, the reader is referred to Volume 45 in its entirety: Melson, Rabinowitz, et al., 1979a), it must be borne in mind that the recovery in Hole 395A averaged only 19%. As pointed out by the Leg 45 scientific party (Melson, Rabinowitz, et al., 1979b), the recovery varied with lithology, the aphyric pillow basalts giving the lowest average recovery (8 and 7% for A_2 and Lithologic Unit 16 of A_3, respectively), the phyric pillow basalts a higher recovery (13% for Units P_3, P_4, and P_5), and the massive basalts a much higher recovery (32% for Unit P_2). Near the base of the hole, where the section has become massive by virtue of annealing, the recovery was high regardless of lithology (19% in the aphyric basalts of Lithologic Units 18 and 19; 40% in the intrusive dolerites of Unit P_4'; 37% in the aphyric basalts of Lithologic Unit 23). Given the low overall recovery, however, and the fact that large sections of the hole were drilled with less than 5% recovery, the unit boundaries must be considered tenuous, and it is likely that several thin units were missed entirely—which, of course, was one of our reasons for logging the hole on Leg 78B.

REFERENCES

Aubouin, J., von Huene, R., et al., 1982. Site 494: Middle America Trench lower slope. *In* Aubouin, J., von Huene, R., et al., *Init. Repts. DSDP*, 67: Washington (U.S. Govt. Printing Office), 27–78.

Boyce, R. E., 1981. Electrical resistivity, sound velocity, thermal conductivity, density-porosity, and temperature obtained by laboratory techniques and well logs: Site 462 in the Nauru Basin of the Pacific Ocean. *In* Larson, R. L., Schlanger, S. O., et al., Init. Repts. DSDP, 61: Washington (U.S. Govt. Printing Office), 743–762.

Cann, J. R., and Von Herzen, R. P., 1983. Downhole logging at Deep Sea Drilling Project Sites 501, 504 and 505, near the Costa Rica Rift. *In* Cann, J. R., Langseth, M. G., Honnorez, J., Von Herzen, R. P., White, S. M., et al., *Init. Repts. DSDP*, 69: Washington (U.S. Govt. Printing Office), 281-300.

Francis, T. J. G., 1982. Large-scale resistivity experiment at Deep Sea Drilling Project Hole 459B. *In* Hussong, D. M., Uyeda, S., et al., *Init. Repts. DSDP*, 60: Washington (U.S. Govt. Printing Office), 841-852.

Hussong, D. M., Fryer, P. B., Tuthill, J. D. and Wipperman, L. K., 1979. The geological and geophysical setting near DSDP Site 395, North Atlantic Ocean. *In* Melson, W. G., Rabinowitz, P. D., et al., *Init. Repts. DSDP*, 45: Washington (U.S. Govt. Printing Office), 23-37.

Kasahara, J., Hussong, D. M., and Sutton, G. H., 1980. A seismic study using ocean-bottom seismometers near the Mid-Atlantic Ridge at 23°N. *Mar. Geol.*, 35:199-218.

Melson, W. G., Rabinowitz, P. D., et al., 1979a. *Init. Repts. DSDP*, 45: Washington (U.S. Govt. Printing Office).

________, 1979b. Site 395: 23°N, Mid-Atlantic ridge, *In* Melson, W. G., Rabinowitz, P. D., et al., *Init. Repts. DSDP*, 45: Washington (U.S. Govt. Printing Office), 131-264.

Montadert, L., Roberts, D. G., et al., 1979. Site 402/Hole 402A. *In* Montadert, L., Roberts, D. G., et al., *Init. Repts. DSDP*, 48: Washington (U.S. Govt. Printing Office), 125-164.

Natland, J. H., 1979. Comparison of chemical and magnetic stratigraphy of DSDP Sites 332 and 395. *In* Melson, W. G., Rabinowitz, P. D., et al., *Init. Repts. DSDP*, 45: Washington (U.S. Govt. Printing Office), 657-677.

Purdy, G. M., Rabinowitz, P. D., and Schouten, H., 1979. The Mid-Atlantic Ridge at 23°N: Bathymetry and magnetics. *In* Melson, W. G., Rabinowitz, P. D., et al., *Init. Repts. DSDP*, 45: Washington (U.S. Govt. Printing Office), 119-128.

Rabinowitz, P. D., and Ludwig, W. J., 1980. Geophysical measurements at candidate drill sites along an east-west flow line in the central Atlantic Ocean. *Mar. Geol.*, 35:243-275.

Raitt, R. W., 1963. The crustal rocks. *In* Hill, M. N. (Ed.), *The Sea* (Vol. 3): New York (Wiley), 85-102.

Salisbury, M. H., Stephen, R., Christensen, N. I., Francheteau, J., Hamano, Y., Hobart, M., and Johnson, D., 1980. The physical state of Cretaceous oceanic crust from the results of logging, laboratory studies, and the oblique seismic experiment at Deep Sea Drilling Project Sites 417 and 418. *In* Donnelly, T., Francheteau, J., Bryan, W., Robinson, P., Flower, M., Salisbury, M., et al., *Init. Repts. DSDP*, 51, 52, 53, Pt. 2: Washington (U.S. Govt. Printing Office), 1579-1597.

Stephen, R. A., 1983. The oblique seismic experiment on DSDP Leg 70. *In* Cann, J. R., Langseth, M. G., Honnorez, J., Von Herzen, R. P., White, S. M., et al., *Init. Repts. DSDP*, 70: Washington (U.S. Govt. Printing Office), 301-308.

Stephen, R. A., Johnson, S., and Lewis, B., 1983. The oblique seismic experiment on Deep Sea Drilling Project Leg 65. *In* Lewis, B. T. R., Robinson, P. T., et al., *Init. Repts. DSDP*, 65: Washington (U.S. Govt. Printing Office), 319-328.

Stephen, R. A., Louden, K. E., and Matthews, D. H., 1980. The oblique seismic experiment on Deep Sea Drilling Project Leg 52. *In* Donnelly, T. W., Francheteau, J., Bryan, W., Robinson, P. T., Flower, M., Salisbury, M., et al., *Init. Repts. DSDP*, 51, 52, 53, Pt. 1: Washington (U.S. Govt. Printing Office), 675-704.

Sutton, G. H., Maynard, G. L., and Hussong, D. M., 1971. Widespread occurrence of a high velocity basal layer in the Pacific found with repetitive sources and sonobuoys. *In* Heacock J., (Ed.), *Physical Properties of the Oceanic Crust*, Am. Geophys. Union Monogr., 14:193-210.

van Andel, T. H., and Bowin, C. O., 1968. Mid-Atlantic Ridge between 22° and 23° north latitude and the tectonics of mid-ocean rises. *J. Geophys. Res.*, 73:1279-1298.

Von Herzen, R. P., Francis, T. J. G., and Becker, K., 1983. *In situ* large-scale electrical resistivity of ocean crust, Hole 504B. *In* Cann, J. R., Langseth, M. G., Honnorez, J., Von Herzen, R. P., White, S. M., et al., *Init. Repts. DSDP*, 69: Washington (U.S. Govt. Printing Office), 237-244.

Zoback, M. D., and Anderson, R. N., 1983. Permeability, underpressures, and convection in the oceanic crust at Deep Sea Drilling Project Hole 504B. *In* Cann, J. R., Langseth, M. G., Honnorez, J., Von Herzen, R. P., White, S. M., et al., *Init. Repts. DSDP*, 69: Washington (U.S. Govt. Printing Office), 245-254.

Date of Initial Receipt: September 20, 1983
Date of Acceptance: October 5, 1983

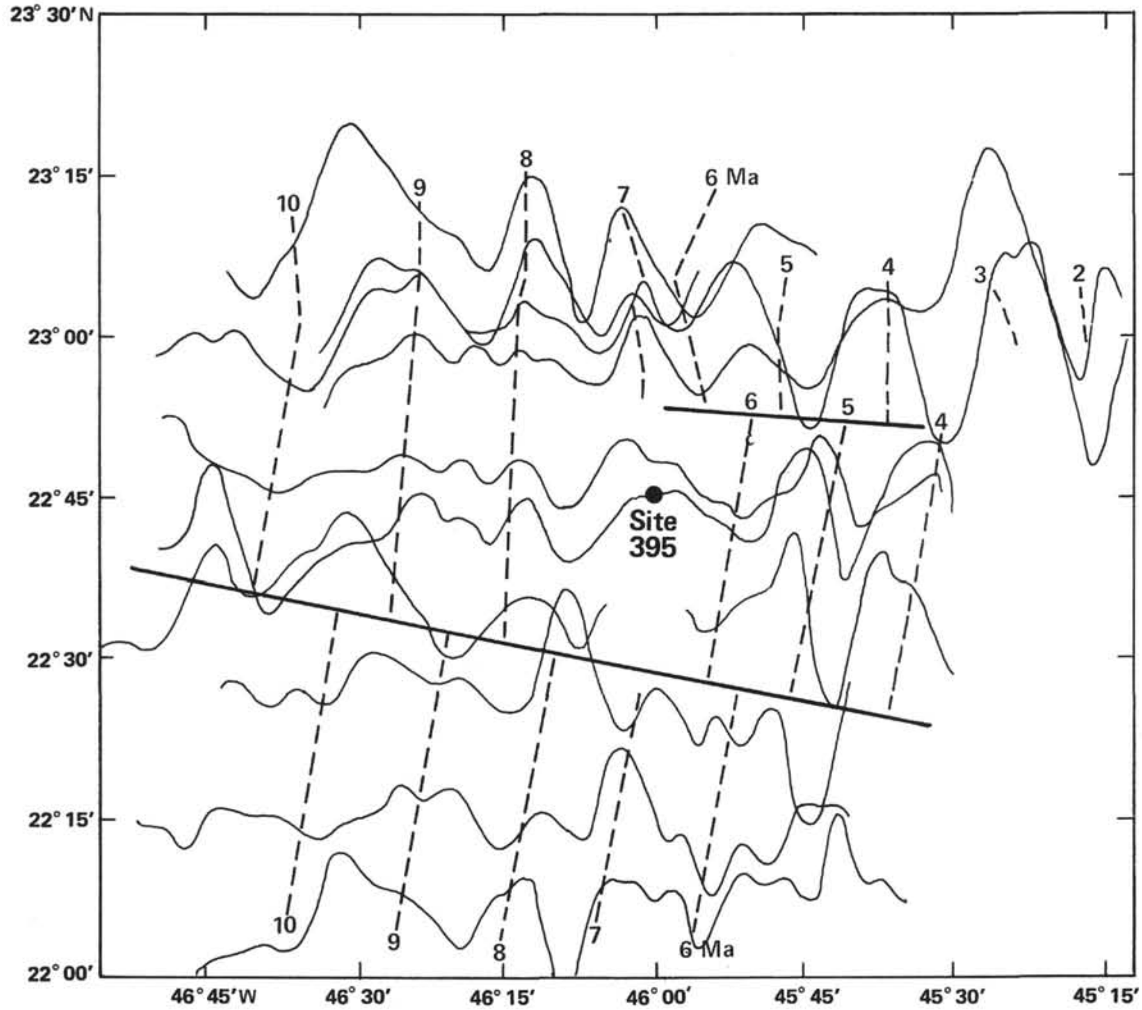

Figure 7. Magnetic anomalies and isochrons in the vicinity of Site 395 (from Hussong et al., 1979). Solid lines show tentative locations of fracture zones. Ages shown in Ma.

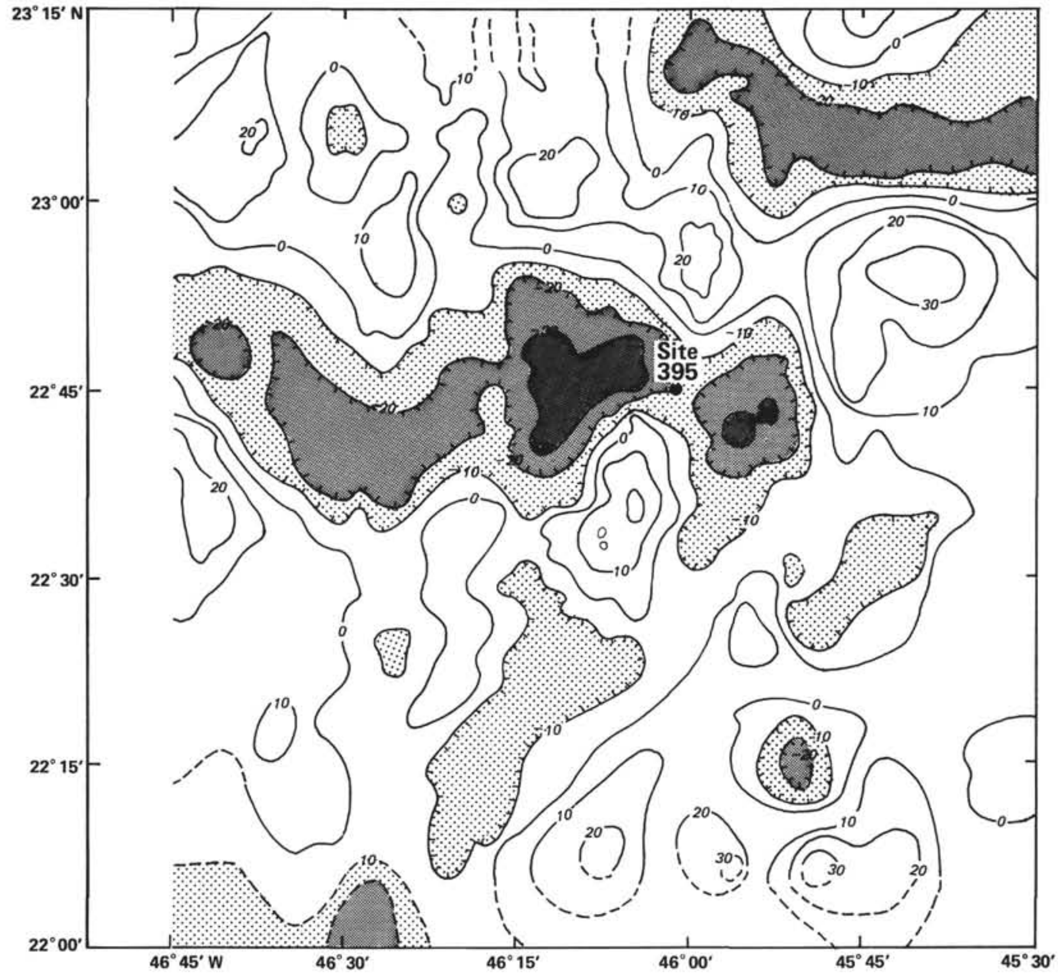

Figure 8. Free-air anomaly map in the vicinity of Site 395 (from Hussong et al., 1979). Values shown in milligals.

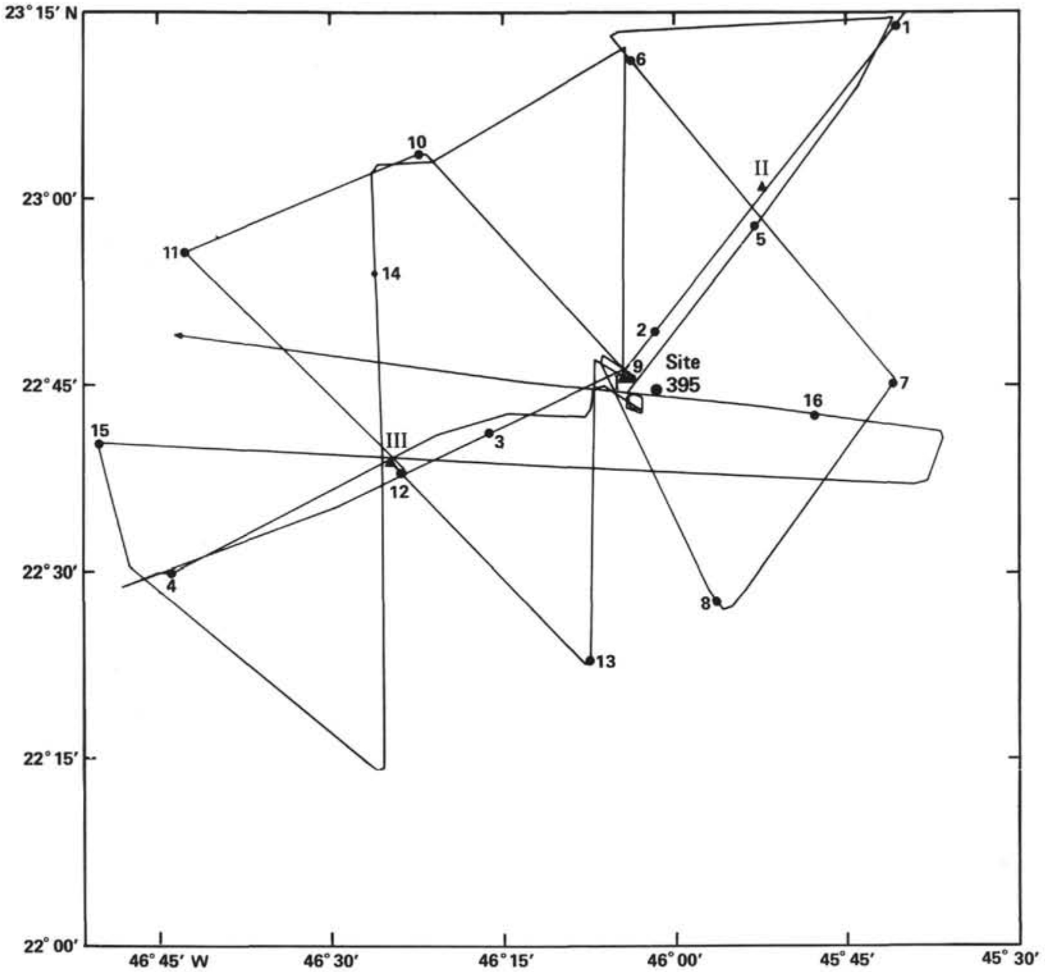

Figure 9. Refraction lines run during site survey in the vicinity of Site 395 (from Hussong et al., 1979). Sonobuoy locations are numbered 1 through 16; of the three ocean-bottom seismometers (I–III) deployed, only OBS I functioned properly.

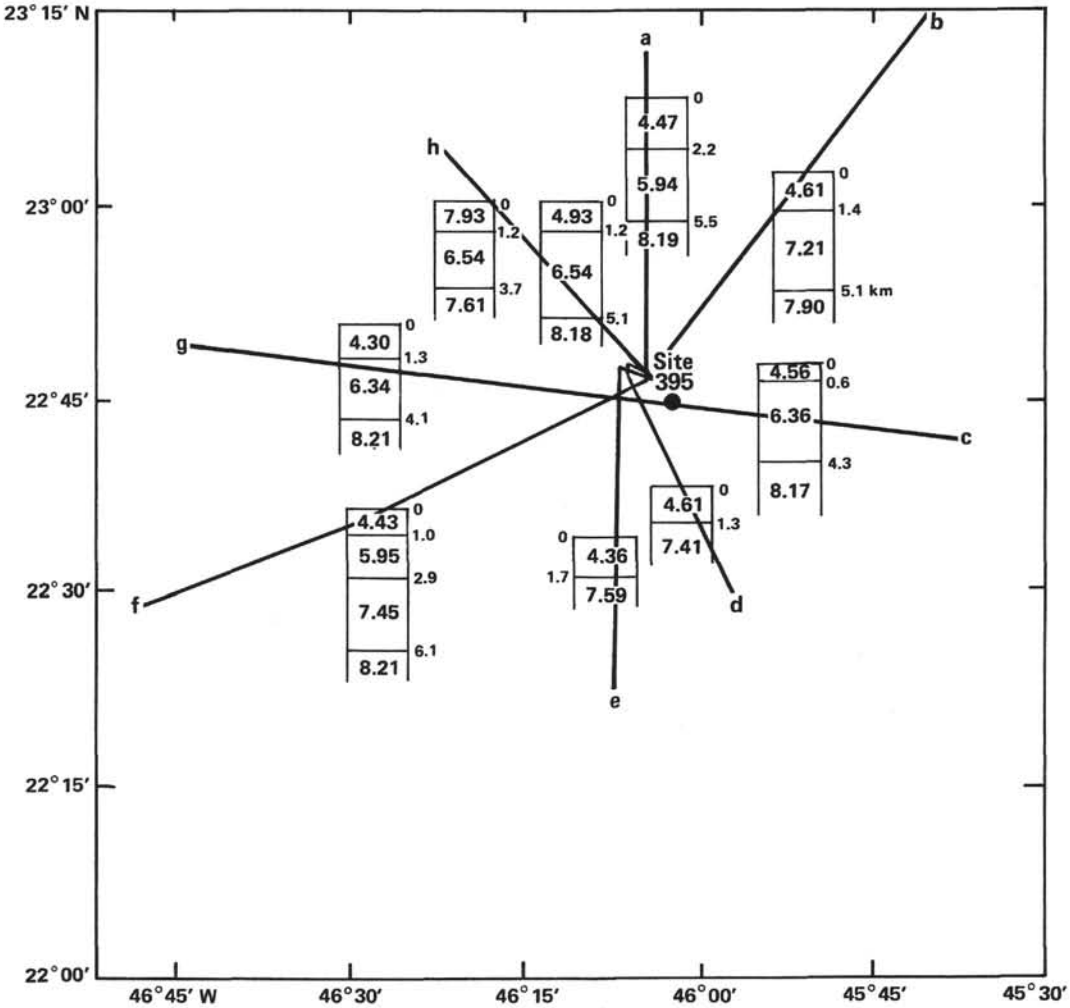

Figure 10. Crustal velocity models obtained along shot lines shown in Figure 9 (from Kasahara et al., 1980). Velocities in km/s. Small numbers indicate sub-bottom depths in km.

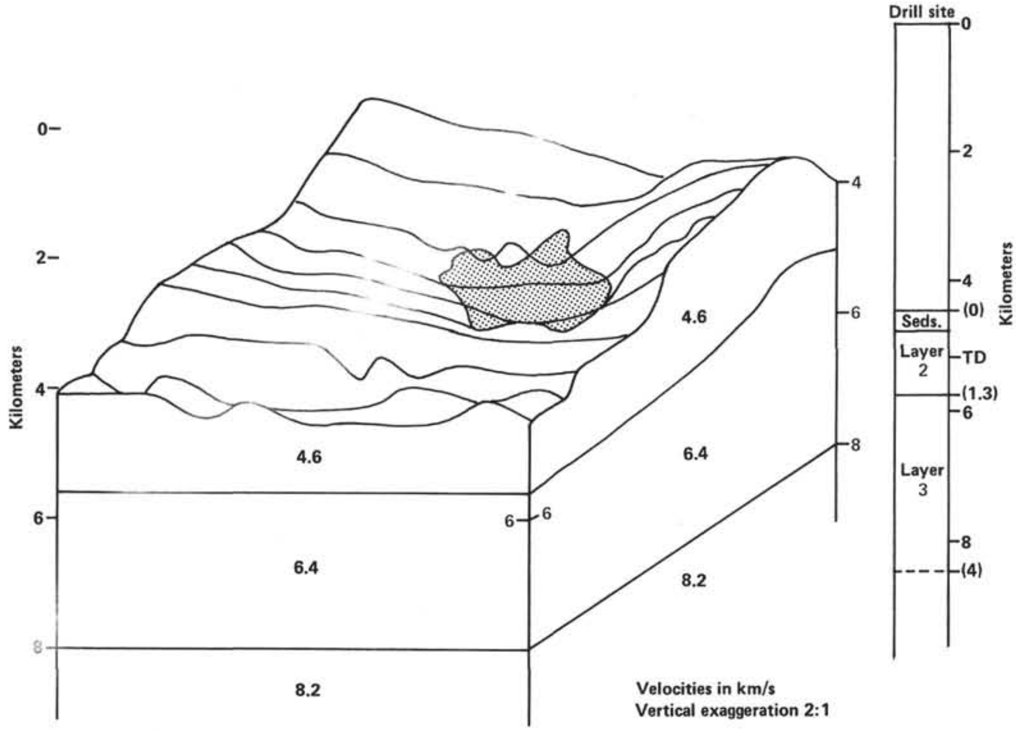

Figure 11. Seismic velocity structure in the vicinity of Site 395 (after Hussong et al., 1979; Kasahara et al., 1980). Numbers in parentheses represent depths sub-bottom.

Table 2. Lithologic summary, Hole 395A.[a]

Lithologic unit	Chemical unit	Lithology	Cores	Inferred sub-bottom interval (m) and thickness (in paren.)	Distinguishing characteristics
1		Sedimentary breccia	3-5	87.60-110.79 (23.19)	Sub-rounded to angular fragments of aphyric basalt, and ultramafic to mafic plutonic rocks in foraminifer-nannofossil ooze
2	A_2	Aphyric basalt	5-13	110.79-172.44 (61.65)	Aphyric pillow basalt
3	—	Sedimentary breccia	13	172.44-174.31 (1.87)	Two sub-angular fragments of serpentinite, 1 pc. aphyric basalt
4	P_2	Phyric basalt	13-16	174.31-210.52 (36.11)	Plagioclase-olivine phyric fine-grained massive basalt
5	P_3	Phyric basalt	17-22	210.52-257.00 (46.48)	Plagioclase-olivine-clinopyroxene phyric
6	—	Phyric basalt	22	257.00-260.37 (3.37)	Plagioclase-olivine-clinopyroxene phyric with fewer plagioclase phenocrysts than Unit 5
7	P_4	Phyric basalt	23-25	260.37-288.79 (28.42)	Plagioclase-olivine phyric with rare large clinopyroxene phenocrysts
8		Phyric basalt	26-27	288.79-307.84 (19.05)	Plagioclase-olivine clinopyroxene phyric
9	—	Phyric basalt	28	307.84-317.34 (9.50)	Plagioclase-olivine phyric
10		Phyric basalt	29	317.34-326.87 (9.53)	Plagioclase-olivine-clinopyroxene phyric pieces and plagioclase-olivine phyric pieces
11		Phyric basalt	30	326.87-336.06 (9.19)	Olivine-plagioclase phyric
12	P_5	Phyric basalt	31	336.06-344.46 (8.40)	Mixed pieces plagioclase-olivine-clinopyroxene phyric and plagioclase-olivine phyric
13	—	Basaltic breccia	32	344.46-354.00 (9.54)	Angular clasts of fine- to medium-grained plagioclase-olivine phyric basalt in carbonate clay-rich matrix; clasts include coarsest-grained basalt found; evidence of hydrothermal alteration
14		Phyric basalt	33	354.00-360.87 (6.87)	Mixed pieces plagioclase-olivine-clinopyroxene and plagioclase-olivine phyric basalt
15		Hyaloclastite	33	360.87-362.24 (1.37)	Fine-grained basalt and basaltic glass in recrystallized carbonate ooze
16		Aphyric basalt	33-49	362.24-504.77 (142.53)	Aphyric basalt with very rare rounded plagioclase "xenocrysts"
17	A_3	Basaltic breccia	49	504.77-508.74 (3.97)	Angular, brecciated fine- to medium-grained basalt clasts, including variolitic rinds and altered glass clasts in clay-rich matrix
18	— b	Aphyric basalt	49-58	508.74-585.00 (76.26)	Aphyric basalt with rare olivine and plagioclase "xenocrysts," highly fractured, abundant veins filled with secondary minerals
19	A_4 —	Glass-rich basaltic breccia and aphyric basalt	58-61	585.00-608.10 (23.10)	Breccias with abundant basaltic glass marginally altered to numerous secondary minerals in a matrix of alteration products; some zones of aphyric basalt with some glassy rinds with variolitic zones
20		Dolerite	61	608.10-617.49 (9.39)	Plagioclase-olivine-clinopyroxene basalt, medium-grained
21	$P_{4'}$	Aphyric basalt	62	617.49-617.96 (0.47)	Thin zone of aphyric basalt with glassy and variolitic rind; surfaces sheared and coated with clay and other secondary minerals
22	—	Dolerite	62-64	617.96-630.15 (12.19)	Plagioclase-olivine-clinopyroxene basalt, medium-grained; quenched contact at base
23	A_4	Aphyric basalt with some glassy breccia zones	64-67+	630.15-664.09+ (33.94+)	Aphyric basalt, glassy basaltic breccias, numerous glassy-variolitic rinds, abundant soft light-colored clay in fractures; highly fractured

[a] Note: Taken from Melson, Rabinowitz, et al. (1979b).
[b] The boundary between Chemical Units A_3 and A_4 lies within Lithologic Unit 18 at a sub-bottom depth of 570.08 m.

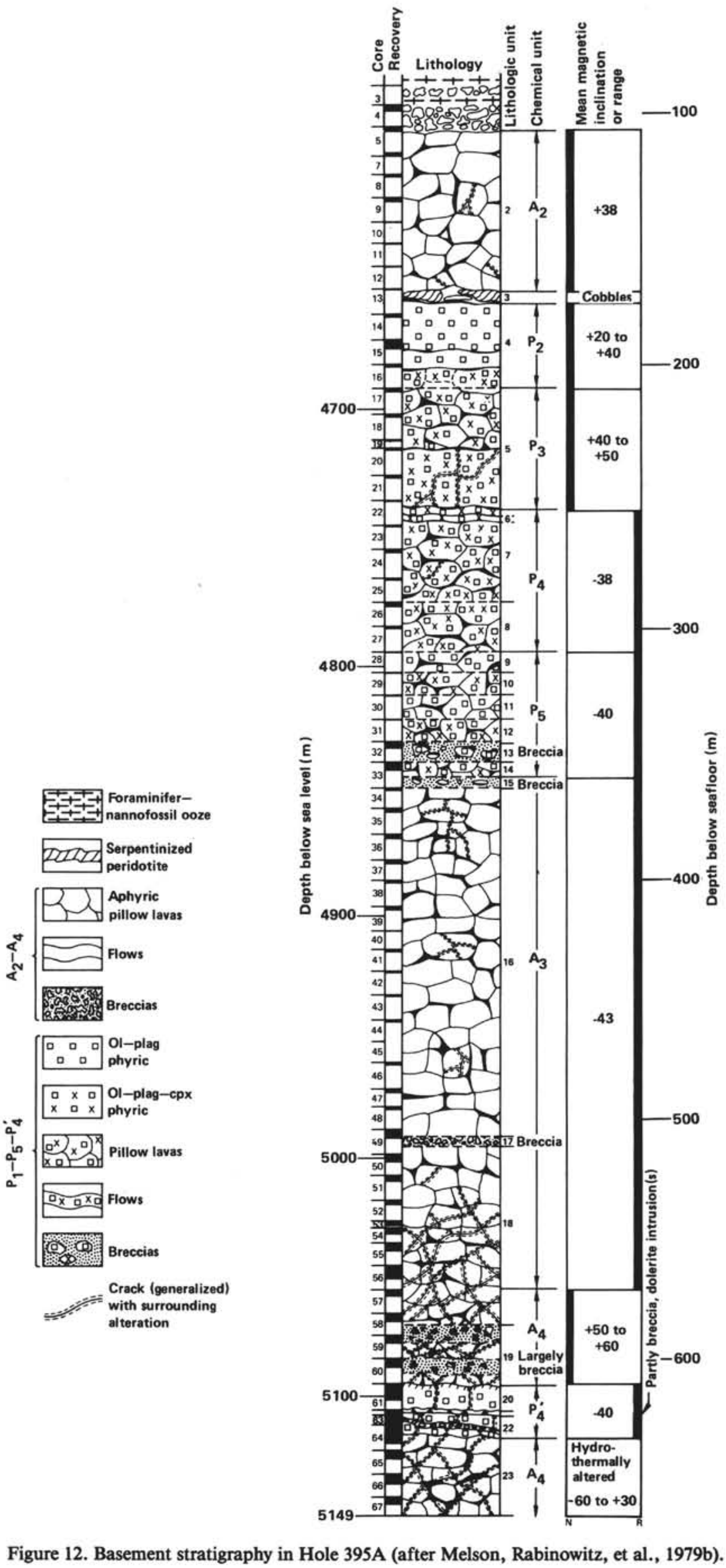

Figure 12. Basement stratigraphy in Hole 395A (after Melson, Rabinowitz, et al., 1979b).